Cell adhesion phase separation and force remodeling heterogeneity modulate nuclear spatial force-sensing mechanobiology on microarrays

Introduction:
Bioengineered microarrays provide a powerful platform for controlling cell morphology and mechanical signaling. However, how microarray-induced adhesion phase separation and force heterogeneity influence nuclear force-sensing mechanotransduction remains poorly understood. This study aimed to elucidate how microarray-mediated cell adhesion heterogeneity modulates cytoskeletal remodeling, mechanical stress distribution, and nuclear mechanobiology in mesenchymal stem cells (MSCs).

Methods:
Photoreactive biopolymers were synthesized via Steglich esterification and patterned by photolithography into microarrays with distinct aspect ratios (1:1, 4:1, 8:1). MSCs were cultured on these arrays to control cell geometry and adhesion. Focal adhesion (FA) maturation was characterized through integrin, vinculin, and LIMD1 staining, while actomyosin organization and nuclear mechanics were evaluated using AFM nanoindentation, immunofluorescence, and quantitative morphometry. Proteomic profiling was performed via LC-MS/MS and analyzed for force- and adhesion-related proteins regulated by geometric cues.

Results:
Phase-separated focal adhesions preferentially formed along geometric boundaries, generating spatially biased cytoskeletal tension. This heterogeneity induced localized nuclear deformation and anisotropic mechanotransduction, as evidenced by altered LaminA/C, YAP, and Ki67 distributions. Actomyosin contractility and nuclear curvature were significantly correlated with microarray elongation ratio. Proteomic analysis revealed differential expression of proteins involved in adhesion (Integrin, Paxillin, Talin), cytoskeletal remodeling (Actin, Myosin), and nuclear mechanosensing (LaminA/C, TRIP6). KEGG and GO enrichment confirmed pathways related to cytoskeletal regulation, focal adhesion, and mechanosignaling.

Discussion:
These findings demonstrate that engineered microarray topographies modulate cellular nanomechanics by inducing adhesion phase separation and heterogeneous force remodeling. Such microscale mechanical cues reorganize nuclear architecture and regulate spatial mechanotransduction, establishing a direct link between extracellular geometry and nuclear biomechanics.

Significance/Clinical Relevance:
Understanding how phase-separated adhesions and force heterogeneity control nuclear force-sensing provides new mechanistic insights into cellular mechanobiology and stem cell fate regulation. This work establishes a bioengineered microarray platform for studying mechanoresponsive behaviors and offers a basis for developing next-generation mechanobiomaterials for regenerative medicine.

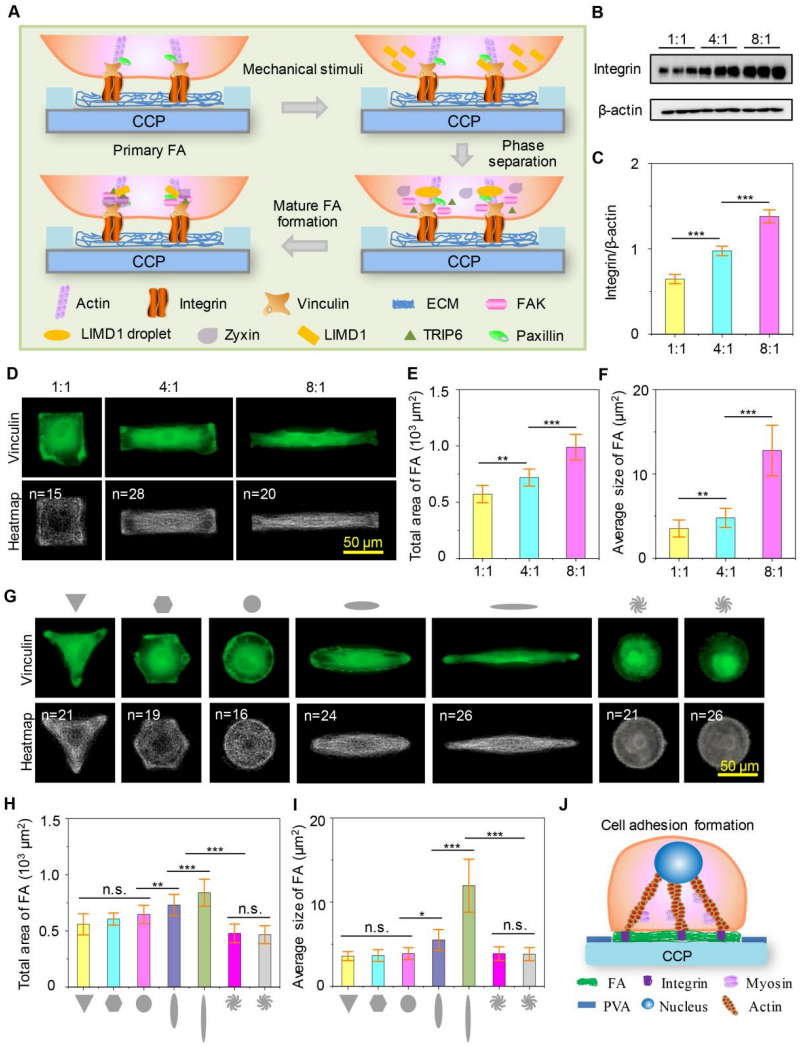

Figure 1. Phase-separated heterogeneous expression of adhesion-related proteins in the microarrayed cells. (A) Illustration of adhesion-related protein phase separation to regulate mature FA formation by mechanical stimuli. The extracellular mechanical cues could mediate vinculin activation by the recruitment of adhesion proteins, including Integrin, Talin, Paxillin, FAK, TRIP6, Zyxin, VASP and Vinculin to induce LIMD phase separation and promote heterogeneous FA formation. (B) WB analysis of Integrin protein on the microarrays. (C) Relative Integrin expression level of MSCs (n = 3 independent experiments). (D) Representative micrographs of vinculin staining in square elongated cells. The heatmap of vinculin is formed by

stacking >15 micrographs along with the z-axis into one image. (E) Total area of FA in the square elongated cells (n = 15 independent experiments). (F) Average size of FA in the square elongated cells (n = 15 independent experiments). (G) Representative micrographs of vinculin staining in geometric, circular elongated and chiral cells. (H) Total area of FA in geometric, circular elongated and chiral cells (n = 15 independent experiments). (I) Average size of FA in geometric, circular elongated and chiral cells (n = 15 independent experiments). (J) Relationship of cell adhesion formation on the microarrays. The data present mean ± SD. n.s., not significant; *p<0.05; **p<0.01; ***p<0.001.

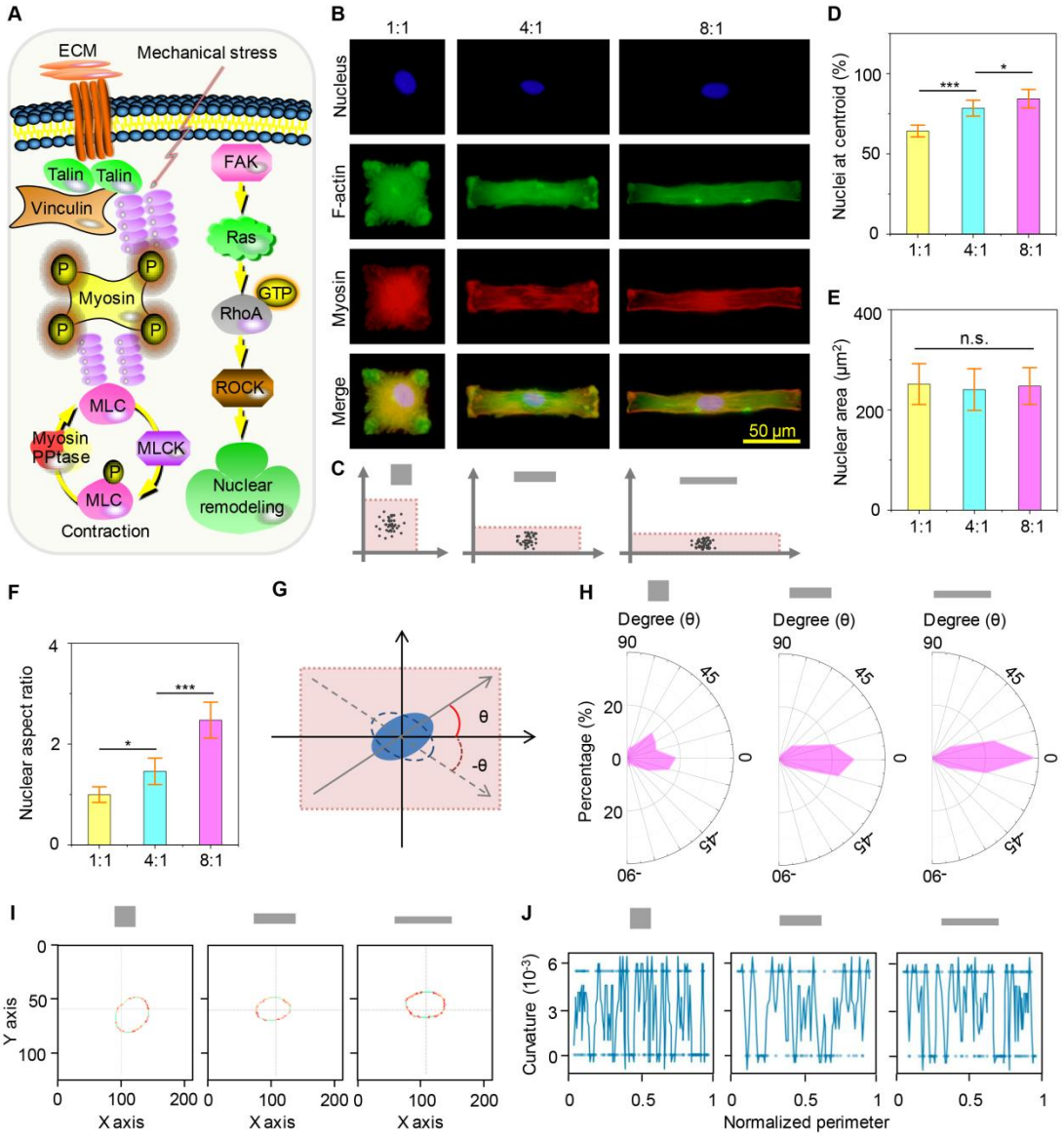

Figure 2. Heterogeneous mechanical stress from biased cytoskeleton force remodeling to supervise nuclear spatial ectopia configuration on the microarrays. (A) Illustration of extracellular stimuli from the biofunctional microarrays to alter nuclear remodeling by cytoskeleton-mediated mechanical stress. (B) Representative micrographs of motor proteins (myosin) staining. Green: myosin; red: actin; blue: nuclei. (C) Discrete nuclear distribution on square elongated microarrays. (D) Nuclei

at centroid (%) in square elongated cells (n = 5 independent experiments). (E) Nuclear area of square elongated cells (n = 50 independent experiments). (F) Nuclear aspect ratio (n = 20 independent experiments). (G) Illustration of nuclei how to calculate nuclear compliant degree. (H) Nuclear compliant degree along with the elongated axis in the microarrayed cells. (I) Nuclear track maps and curvature level of MSCs on the microarrays. (J) Nuclear curvature in the normalized perimeter in square elongated MSCs. The data present mean ± SD. ns, not significant; *p<0.05; ***p<0.001.

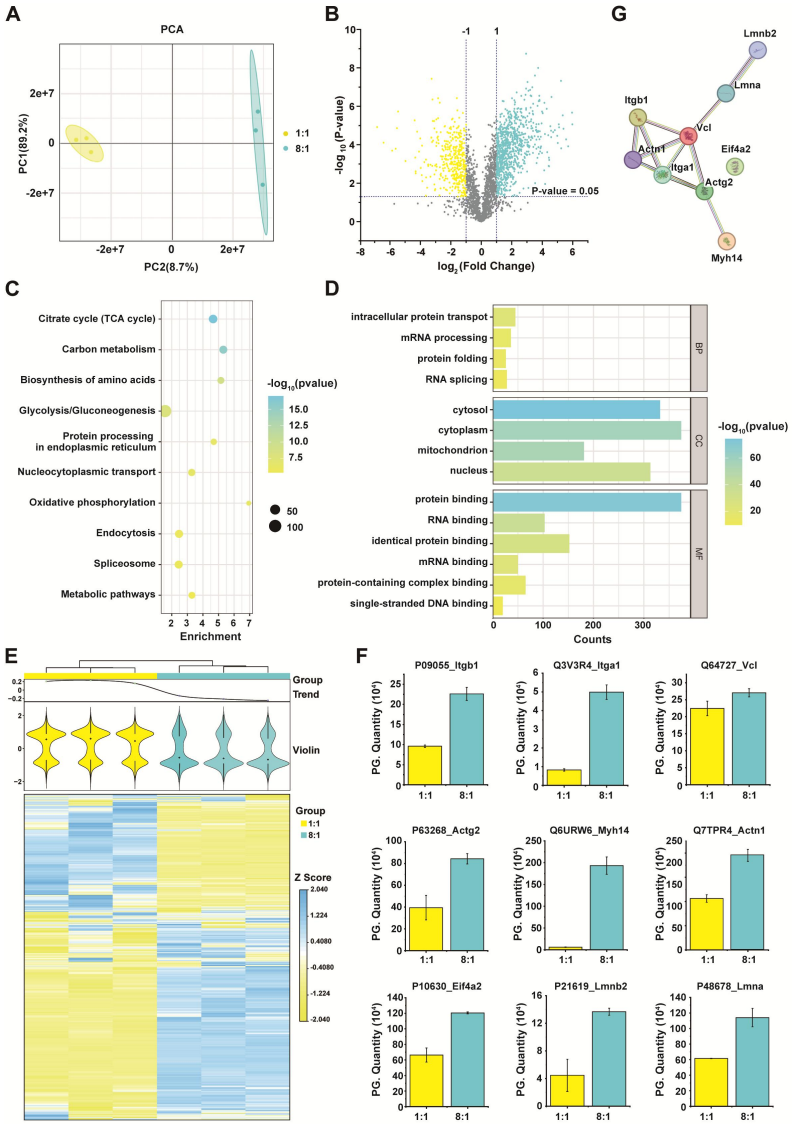

Figure 3. Proteomic analysis of MSCs cultured on microarrays with aspect ratios of 1:1 and 8:1. The analysis was performed in DIA mode using the Thermos Scientific EASY-1200 system (120 min gradient) and Obitrap Explorise 480 mass spectrometer. (A) PCA analysis of the proteins of 1:1 and 8:1 microarray aspect ratios. (B) Volcano plot of differential expression of proteins between 1:1 and 8:1 microarray aspect ratios. Fold change was derived from the protein abundance in the 8:1 over 1:1 microarray aspect ratio. (C) The KEGG enrichment analysis of the

up-regulated proteins in (B). (D) The GO enrichment analysis of of the up-regulated proteins in (B). (E) The heatmap of the proteins of 1:1 and 8:1 microarray aspect ratios. (F) Abundances of significant upregulation proteins related to cell adhesion, cytoskeleton remodeling, nuclear proteins. Boxplots report the 25% (lower hinge), 50% and 75% quantiles (upper hinge). Whiskers indicate observations equal to or outside hinge+/– 1.5* interquartile range (IQR). (G) The protein-protein interaction (PPI) network analysis of the nine proteins identified in (F). The data present mean ± SD. n = 3 independent experiments.